



Morphology, chemical and mineralogical composition of magnetic fraction of coal fly ash

Ewa Strzałkowska

Silesian University of Technology, Faculty of Mining, Safety Engineering and Industrial Automation, Department of Applied Geology, Gliwice, Poland



ARTICLE INFO

Keywords:
Magnetic fraction
Ferrospheres
Ash utilization
Chemical elements
Critical elements

ABSTRACT

The article presents in detail the geochemical and mineralogical characteristics of magnetic particles formed during energetic combustion of hard coal and lignite. The aim of the research was to assess their suitability as a source of possible raw materials necessary for the development of new technologies. Both hard coal and lignite fly ash, as well as the magnetic fractions separated from them, have been tested using various analytical methods.

The chemical composition, phase composition, the size, and morphology of magnetically susceptible particles were determined. The main phases identified in the magnetic fraction are magnetite, hematite, and multicomponent phases, often trapped in aluminosilicate or calcium-aluminosilicate basic glass. In order to compare the chemical composition of the magnetic fractions and raw ashes, EF was calculated - the enrichment factor of the component in the magnetic fraction in relation to ash. Among the elements that have been enriched, apart from Fe, the following should be mentioned: Mg, Mn, Co, Nd, Cu, Ni, and Au. Only the concentrations of Cu and Ni in the magnetic fraction of lignite are much higher than the Clarke value (average concentration in ash), therefore the recovery of these raw materials can only be profitable from this ash. Research confirmed that when choosing the waste for the separation of metal concentrates, the content of the raw material in the ash is not always the most important, but also the form of its occurrence.

1. Introduction

Contrary to popular belief, the by-products of combustion are not only waste but also valuable raw material for other processes (Ahmaruzzaman, 2010; Blissett and Rowson, 2012; Uliasz-Bocheńczyk et al., 2015). Fly ashes are especially valuable. They are the finest, heterogeneous residue after burning coal in boilers. They rise with the flue gases and are captured by electrostatic precipitators, baghouses, or cyclones (Suárez-Ruiz et al., 2017; Galos and Uliasz-Bocheńczyk, 2005). For years, ash has been widely used as a mineral additive in the production of cement, multi-component binders, and concrete (Giergiczny and Gawlicki, 2005; Giergiczny et al., 2013). They are also used for road construction, land reclamation, and underground mining (Galos and Uliasz-Bocheńczyk, 2005). The possibility of managing the ashes is primarily determined by their chemical composition. The presence of a number of metals in the ashes has been demonstrated in many studies (Hycnar, 1987; Vassilev and Vassileva, 1997) including rare earth elements (Seredin, 1996; Dai et al., 2014; Hood et al., 2017; Kolker et al., 2017; Adamczyk et al., 2020). The interest in metal recovery was generally focused on the current production of ash, however, according

to Hower et al. (2017), ash collected in ponds or in landfills can also be a source of valuable elements, primarily rare earth elements.

One of the directions of using fly ash may also be the recovery of magnetically susceptible phases from them. The main components of the magnetic fraction of fly ash are iron minerals: magnetite and hematite (Hower et al., 1999; Xue and Lu, 2008; Strzałkowska, 2011; Wei et al., 2017), and to a lesser extent quartz and mullite (Lu et al., 2009; Wang, 2013). Komraus et al. (2003) found the presence of the superparamagnetic phases of hematite in addition to magnetite and hematite in fly ash of medium and small particle diameters. The content of iron oxides in the ashes is variable and depends, among others, on the content of iron in coal, where it occurs mainly in the form of sulphides (pyrite and marcasite) and carbonates (Gabzdyl, 1987). According to Flanders (1994), an increase in the content of sulphides in coal by 1% by weight causes an increase in the content of iron oxides in the ash by 7%. The course of coal combustion, and precisely the amount of oxygen in the combustion chamber, determines the degree of iron oxidation. Since iron oxide Fe_2O_3 (hematite) is a weakly magnetic compound, in order to recover the magnetic fraction, the combustion process in the boiler should be carried out in such a way as to obtain Fe_3O_4 (magnetite). The

E-mail address: ewa.strzalkowska@polsl.pl.

<https://doi.org/10.1016/j.coal.2021.103746>

Received 13 February 2021; Received in revised form 6 April 2021; Accepted 10 April 2021

Available online 20 April 2021

0166-5162/© 2021 Silesian University of Technology. Published by Elsevier B.V. This is an open access article under the CC BY license (<http://creativecommons.org/licenses/by/4.0/>).

highest content of magnetic iron compounds (approx. 10%) was found in ashes of the silicate type, lower in Al-rich ashes, and the lowest in Ca-rich ashes (Hycnar et al., 2012). The influence of the place of collecting fly ash from the electrostatic precipitator on the content of the mentioned components was also examined. The highest contents of the ferromagnetic fraction were found in the ashes from the 1st zone of the electrostatic precipitator (Hycnar et al., 2012).

Due to the fact that forming of magnetite during combustion lasts only a few seconds, its physical properties differ from those of natural magnetite, formed during long lasting crystallization. The magnetite created in the combustion process has greater porosity than the natural magnetite, as a result of which it has a lower density, lower magnetic susceptibility, and slightly lower hardness (Michaliková et al., 1994). Optical studies of the magnetic fraction of fly ash showed that magnetite is generally a component of spherical aggregates, the so-called ferrospheres (Jónczy et al., 2012). In addition to Fe_3O_4 magnetite, the presence of the following was found: $\alpha\text{-Fe}_2\text{O}_3$ hematite, $\gamma\text{-Fe}_2\text{O}_3$ maghemite, Al—Mg spinels, wüstite, pyrrhotite, and metallic Fe (Ratajczak and Piestrzyński, 2000). Ferrous phases usually coexist with glass, mostly aluminosilicate, and in lignite coal ashes, also alkaline and ultra-alkaline (Sokol et al., 2002). Most ferrospheres have a dendritic or skeletal structure. According to Sokol et al. (2002), the crystallization of ferro-spinel in ferrospheres occurs as a result of the change of Fe^{2+} to Fe^{3+} . According to Ratajczak and Piestrzyński (2000) and Strzałkowska (2011), the size of spherical aggregates does not exceed 300 μm , while the size of single crystals is usually 1–8 μm . Interest in ferrospheres results from the fact that not only do they have magnetic properties, but are also characterized by high thermal stability and mechanical strength (Sharonova et al., 2013). Ferrospheres have also been used as an effective catalyst for oxidative conversion of methane (Anshits et al., 2000).

In the fuel industry, compounds containing iron oxides are increasingly used as catalysts for the reduction of nitrogen oxides NO_x from flue gases, or as catalysts for the oxidation of soot. The main advantage, apart from their high catalytic activity, is that they are ecological and cheap. As shown in the above-mentioned examples, iron oxides play and will probably continue to play a significant role in many sectors of the economy in the coming years. Therefore, it can be assumed that the separation of the magnetic fraction from the fly ash may expand the sources of this particular metal. Moreover, the chemical composition tests showed that the magnetic fraction of fly ash, in comparison to non-magnetic fractions, is characterized not only by a higher concentration of iron, but also a 2–4 times higher concentration of cobalt, nickel, and manganese (Kukier et al., 2003). The enrichment of the magnetic fraction in heavy metals was also noted by Lu et al. (2009), De Boom et al. (2011), Wang (2013), Wei et al. (2017), and Bielowicz et al. (2018).

Some of these metals have been included by the European Commission (September 3, 2020) in the group of critical raw materials necessary for the development of new technologies. An example of a critical raw material could be cobalt, as the EU will need around 15-times more of it in 2050. It is also worth emphasizing that for the European economy in times of the pandemic, all raw materials are important, not only those classified as critical. The COVID-19 crisis has revealed just how disrupted the supply of raw materials can be. So, recycling becomes the most important thing, not only at present, but also in the future. In order to obtain the best possible effect of recovering individual raw materials from fly ash, knowing the form in which these raw materials occur is essential to recycle them. Therefore, the main aim of the study was geochemical and mineralogical characteristics of magnetic particles formed during energetic combustion of hard coal and lignite. It will not only increase the waste management rate, but also improve the properties of “cleaned” ash.

2. Materials and methods

For the purpose of this study, the magnetic fractions (WKM and WBM) of Class F fly ashes (of hard coal) and Class C fly ashes (of lignite)

from power plants in Poland were tested. These fractions were separated from the ash manually, with dry method, using a magnet. The chemical and phase composition were determined. The content of main and trace elements was determined both in raw ashes and in the separated magnetic fraction of these ashes. The tests were carried out in a laboratory (Bureau Veritas Mineral Laboratories) in Canada using the ICP-AES and ICP-MS methods. All samples were analysed by Lithium Borate Fusion. The phase composition of the studied magnetic fractions was determined using the PANalytical Empyrean X-ray diffractometer using filtered cobalt radiation in a Pixedet detector configuration. A sample of approximately 0.5 g was used to perform the qualitative phase analysis. The phase composition was identified in accordance with the accredited M1-RTG procedure and the International Center for Diffraction Data PDF-4+, version 2020 database. The quantitative analysis was performed using the Rietveld method.

The separated magnetic fractions were also examined in terms of particle size and shape with the use of dynamic image analysis using the QICPIC measurement sensor from Sympatec GmbH based on the ISO 13322-2: 2006 standard. The morphology of magnetic particles was observed using the Axioplan reflected light microscope from Zeiss at 200 and 500 \times magnification and the JSM 7200F Scanning Electron Microscope (SEM) from JEOL equipped with Octane Elite Super EDS detector from EDAX. A microanalysis of the chemical composition of the observed particles was performed using the EDS detector in randomly selected fields, placed representatively over the entire surface of the sample. The tests were carried out using an accelerating voltage of 15 kV.

3. Results

3.1. Granulometric composition and morphology of particles

The size of the particles has a significant influence on their possible further use. Taking this aspect into account, the assessment of the particle size distribution of the magnetic fraction of both ashes was carried out using the QICPIC / R measuring sensor, whose optical system enables the analysis of dynamically changing images. The obtained signals were used to calculate the particle size distribution and to determine the frequency of occurrence of selected grain classes. The results of the analyses are presented in Fig. 1.

The shape of curves for WKM sample indicates an asymmetric (left-skewed) particle size distribution with a clearly marked maximum for particles of approx. 120 μm . For WBM the curve was close to symmetrical with a more blurred maximum for particles in the range of 40–90 μm . The differences in the grain size of the samples are significant. WKM has a larger grain size, as 55% of the particles of this fraction have a particle diameter above 100 μm , while in WBM these particles constitute only 20%.

The sphericity of particles was also determined by determining the AR (Aspect Ratio). For perfectly spherical particles, the value of AR is equal to 1. The course of the cumulative curves (Fig. 2) indicates a greater sphericity of WKM particles, because 32% of the ash particles have an AR greater than 0.9, while for WBM it is less than 9%.

3.2. Chemical composition

The chemical composition of the tested ashes and their magnetic fractions is presented in Figs. 3 and 4. The above results clearly show that the basic factor influencing the chemical composition of fly ash is the type of basic fuel used (in this case, hard coal and lignite). According to the standard, the ash resulting from the combustion of hard coal (WK) is silicate-rich.

The main components of this ash are silicon dioxide SiO_2 and aluminum oxide Al_2O_3 , the following occur in minority: Fe_2O_3 , MgO , CaO , Na_2O , K_2O and TiO_2 . The ash resulting from the combustion of the lignite (WB) is characterized by a different chemical composition. The

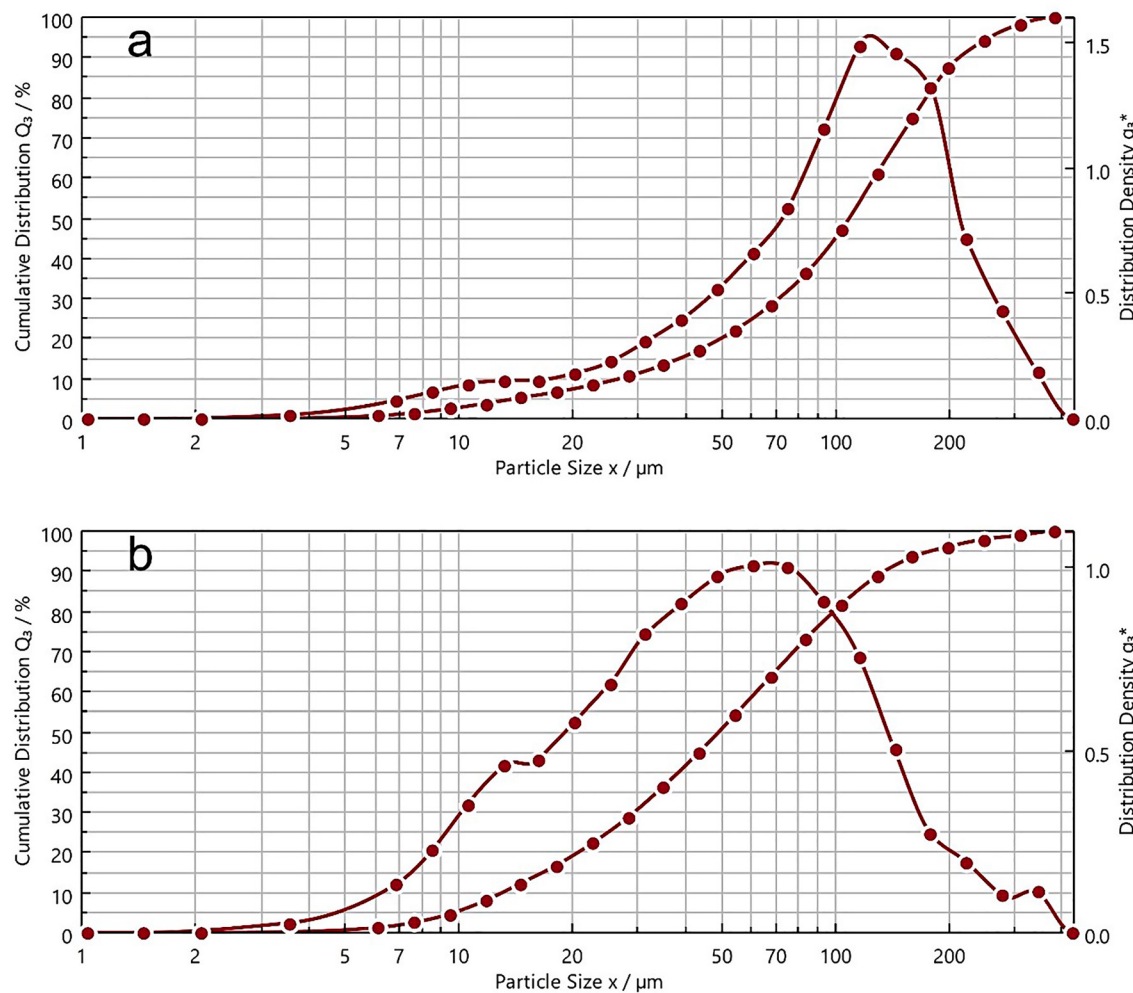


Fig. 1. Particle size distribution – cumulative Q and density q magnetic fraction of class F fly ash (WKM) b) magnetic fraction of class C fly ash (WBM).

SiO_2 content was around 1.5-times lower than its content in WK and the CaO content was simultaneously increased by eight times, which makes it possible to classify this material as calcium-rich ash. In the context of the considered problem, it is noteworthy that the iron Fe_2O_3 content was almost twice that of its content in WK sample.

Comparing the concentration of basic components in the magnetic fractions and the raw ashes, we notice a 10-fold increase in iron content and a minimal increase in magnesium content in the WKM sample, and a significantly lower, 5-fold increase in iron content in the WBM, despite the higher concentration of this element in the initial sample. The explanation for such a large difference in the enrichment of both materials was provided by subsequent studies.

The concentrations of trace elements in the tested ashes and their magnetic fractions were also determined and compared. The results are presented in Table 1. Bearing in mind that the content of trace elements in the ash depends on their content in coal, which depends on the type of coal and the place of origin, it can be concluded that the concentrations of the above-mentioned elements are similar, but often slightly higher in lignite ash. This applies especially to the elements of the lanthanide series, as well as most heavy metals (Pb , Zn , Ni , As , Cd , Hg).

Similar results were obtained by Wdowin and Franus (2014). This slightly higher concentration of rare earth elements in WB may be due to the presence of unidentified phosphate phases in this sample, as indicated by the simultaneous presence of phosphorus and calcium (Mishra et al., 2019). The higher concentration of As , Cd , Hg , Ni , and Pb in WB compared to WK is probably correlated with the higher concentration of sulfur in this sample. It may also be related to the higher share of fine

grains in the WB sample. The correlation between the concentration of trace elements in ashes, and its granulometric composition has already been noticed by Martinez-Tarazona and Spears (1996).

A distinctly different tendency was observed for rubidium. The concentration of this element was 16-times higher in WK (157.1 ppm) than in WB (9.9 ppm). This element is geochemically similar to potassium, its primary source is probably the potassium minerals present in hard coal (Kabata-Pendias and Pendias, 1999). An increased content of K_2O (2.84%) was found in the WK sample, therefore rubidium is probably a component of the glass phase or of the thermally unchanged illite phase of WK ash.

The concentrations of the researched elements in the ash and the magnetic fraction were also compared by calculating EF - enrichment / depletion factor of the component in the magnetic fraction compared to the raw ash. Fig. 5 shows only those cases where a significant enrichment was observed in at least one of the fractions ($\text{EF} \geq 1.3$).

Among the trace elements that were concentrated in the magnetic fraction, the following should be mentioned: Co, Nd, Cu, Ni and Au. According to the geochemical classification of Goldschmidt (1922), they are mostly siderophilic elements. Similar results were obtained by Vassilev et al. (2004). The enrichment factor, however, did not correlate with the iron content in these samples. Already in the 1980s, the relation between Cd, Ni, Co and the magnetic phase were highlighted in the work (Hulett, 1980). According to the authors, the internal structure of the crystal lattice of magnetite and various types of ferrites formed at high temperatures favours the inclusion of numerous elements in it. This enrichment can be explained by the similarity of the ionic radii of the

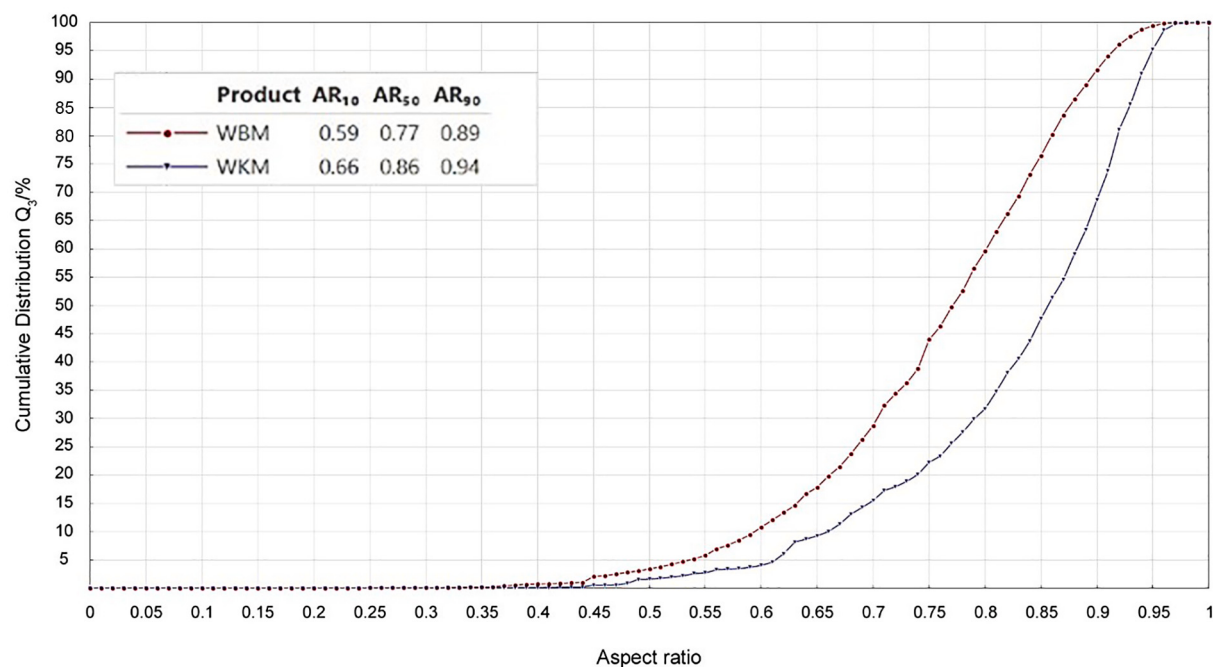


Fig. 2. Cumulative curves picturing the content of grains in the samples with a certain aspect ratio AR.
WKM - magnetic fraction of class F fly ash, WBM - magnetic fraction of class C fly ash.

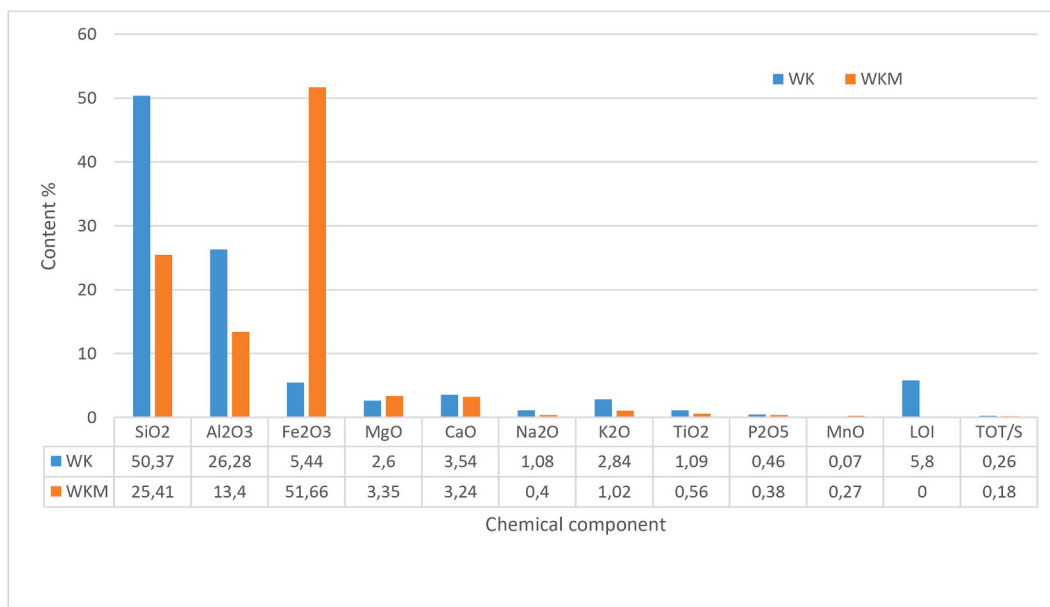


Fig. 3. Chemical composition of WK and WKM.

above-mentioned elements, which favours simultaneous crystallization with iron oxides. Recent studies by Liu et al. (2020) show that Ni and Cu are present in fly ashes in a range of particles with a size of 2–15 µm. Ni occurs mainly in Fe oxides and as NiO, while Cu mainly as Cu₂O / CuO or in Fe oxides. Cu (I) is the dominant oxidation state for Cu.

A surprisingly high enrichment factor is observed for Au (for WKM - EF > 16.4, and for WBM - EF > 31.8). Some Au can be organically bound (halogen-organic), the Au primary carrier in coal can also be pyrite (Seredin, 2007; Dai et al., 2012; Seredin and Dai, 2014). Gold and pyrite are formed in similar conditions, gold often forms inclusions in the pyrite. The mechanism of Au concentration with other minerals, however, is still not fully understood and requires further research (Finkelman

et al., 2019). According to Seredin and Dai et al. (2014), during combustion Au probably behaves like highly volatile elements. It volatilizes in the high-temperature zone (1200–1400 °C) and then condenses on the surface of the combustion products, in particular on the surface of glass spheres, most of which remain in the non-magnetic fraction. None of the volatile elements, e.g. (As, Pb, Sb, W), except for Au, was enriched in the magnetic fraction, so the mechanism of their concentration was probably as described by Seredin and Dai et al. (2014). These elements probably condensed on the surface of the glass spheres and are in the non-magnetic fraction. It must therefore be concluded that the Au concentration mechanism must have been different in this case. The above results should be verified by other independent methods on a

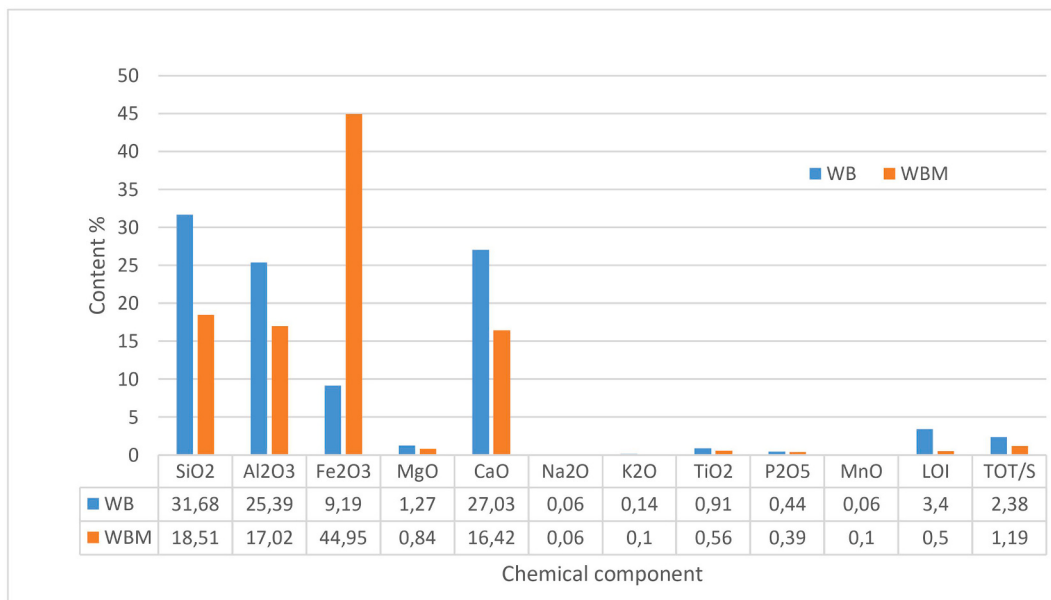


Fig. 4. Chemical composition of WB and WBM.

Table 1

Concentrations of trace elements (ppm) in the tested fly ash samples (WK, WB) and their magnetic fractions (WKM, WBM).

Sample	Be	Co	Cs	Ga	Hf	Nb	Rb	Sn	Sr	Ta	Th
WK	10	37.7	21.1	35	5.6	21.3	157.1	8	578.4	1.7	25.5
WKM	5	89.4	6.7	31.8	2.7	13.2	51.4	6	355.8	0.7	14.4
WB	< 1	42.0	2.6	34.5	5.9	22	9.9	7	586.1	1.5	24.4
WBM	3	138	1.5	22.5	4	14.3	6.5	3	387.8	0.9	17.6
Sample	U	V	W	Zr	Y	La	Ce	Pr	Nd	Sm	Eu
WK	9.8	235	5.2	210.2	48.2	61.8	122.4	14.13	53.5	10.78	2.35
WKM	8.2	204	4	105.1	32.2	34.3	68	8.72	270.1	6.58	1.44
WB	14.5	274	2.7	208.3	92.7	113.5	197	24.05	90.6	17.33	3.66
WBM	10.6	208	1.6	134	67.2	83	143.2	18	200.8	12.87	2.54
Sample	Gd	Tb	Dy	Ho	Er	Tm	Yb	Lu	Mo	Cu	Pb
WK	9.84	1.51	8.72	1.78	5.27	0.73	4.55	0.69	7.5	59.8	40.4
WKM	6.26	0.95	10.25	1.13	3.13	0.47	3.04	0.43	6.8	148.5	14.3
WB	16.07	2.42	13.76	2.79	7.76	1.06	6.71	1.02	5.4	56.5	54.9
WBM	12.34	1.78	12.58	2.03	5.72	0.79	4.72	0.72	7	839	33
Sample	Zn	Ni	As	Cd	Sb	Bi	Ag	Au	Hg	Tl	Se
WK	166	101	28	0.6	3.9	1.3	0.4	< 0.0005	0.62	0.5	2.1
WKM	86	980	11	0.2	2.9	0.5	0.1	0.0082	0.12	0.3	1.6
WB	206	114	33	4.1	0.4	1.1	0.1	< 0.0005	1.48	0.3	25.4
WBM	213	1049	13.2	3.3	0.3	0.6	0.2	0.0159	0.61	0.3	36.7

larger number of samples.

However, most of the considered elements were depleted in the magnetic fraction in comparison to raw fly ashes. The concentration of Si and Al in the WKM decreased by almost a half and amounted to 25.41 and 13.40%, respectively. Therefore, it should be assumed that the above-mentioned elements were concentrated in the non-magnetic fraction. The lowest value of the enrichment factor (EF - 0.2) was found for mercury, which is certainly related to the high volatility of this element.

In order to determine the profitability of recovering a given element from the magnetic fraction of ashes, the value of the enrichment factor EF_k in relation to Clarke values i.e. the average content of a given element in the ashes (Ketris and Yudovich, 2009)) was determined and compared with the calculated value of the enrichment factor EF. The results are presented in Table 2.

The data contained in Table 2 shows that the content of the mentioned trace elements (Mn, Co, Nd, Cu, Ni, and Au) is higher in the studied magnetic fractions compared to their content in the raw fly

ashes. However, if we compare the value of EF for gold with the value of the EF_k of this element, such values prove the low utility of the considered fractions as a source of this element. The profitability of recovering manganese from WBM or cobalt and copper from WKM would also be low. Whereas very high values of the EF_k for nickel ($EF_k > 20$) and copper ($EF_k > 11$) in the case of WBM confirm the importance of this ash as a potential source of the above-mentioned elements. Particularly promising are the results for nickel, which has been monitored by the European Commission for possible inclusion in the next list of critical raw materials ([http://EUR-Lex - 52020DC0474 - EN - EUR-Lex \(europa.eu\) \(2021\)](http://EUR-Lex - 52020DC0474 - EN - EUR-Lex (europa.eu) (2021)))

3.3. Results of XRD analysis

XRD (Figs. 6-7) and microscopic (Figs. 8-10) analyses were performed to determine in detail the mineralogical composition of the magnetic fraction of the ashes. Both samples contain iron oxides, magnetite in the WKM sample constitutes 41.4% by mass and there is

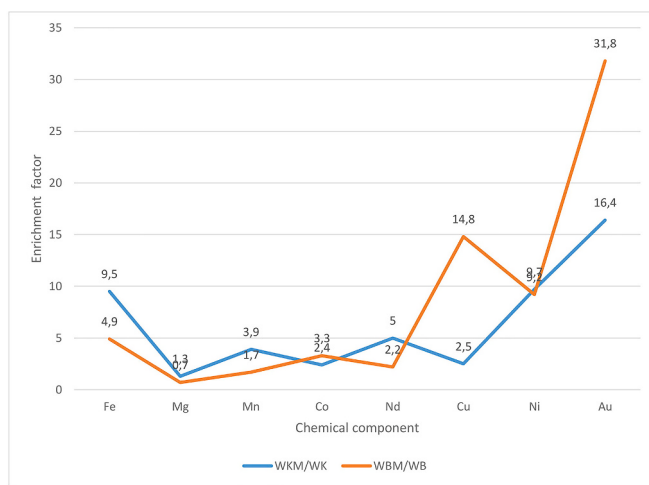


Fig. 5. Enrichment factor values of the components in magnetic fraction compared to raw fly ash.

10% more of it than in the WBM sample. This is one of the reasons why a better enrichment effect was obtained in the WKM magnetic fraction. The content of hematite in both samples is at the same level and amounts to approx. 10% (Table 3). In the WBM sample, iron is also present in brownmillerite. The other components, such as quartz or mullite, are present in smaller amounts. A similar composition of the magnetic fraction of ashes is given in the works of Lu et al. (2009) and Kukier et al. (2003).

The presence of mullite in the sample shows that the combustion temperature in the boiler exceeded 1100 °C. Mullite is mostly crystallized in glass (Vassilev and Vassileva, 2007). The WBM sample is characterized by a more complex phase composition, as the presence of akermanite, anorthite, lime, anhydrite and syngenite was also observed here. This phase composition reflects the high calcium oxide content in this sample. Distribution of CaO in the individual mineral phases is controlled by the availability of SO₃ and free CaO (Enders, 1996).

The amorphous component also has a significant share in both tested samples. Taking into account the measurement error value, it can be assumed that its share in both samples is similar. Judging by the chemical composition and microscopic observations, there are other iron or aluminum spinels in the samples, but magnetite is the only spinel mineral in sufficient quantity to be detected by XRD.

3.4. Microscopic observation

The magnetic phases identified in the XRD analysis were also observed under the microscope in reflected light. Research with the use of the reflected light microscope allowed for the observation of the microstructure of these particles. Most of them were sized between 40 and 100 µm. The magnetic particles were mostly spherical, yet non-spherical forms were also observed, though rarely. Magnetite (grey-white, low-reflectance, isotropic) was the main component of all spherical aggregates (Figs. 8–9), porous in places (Fig. 8a), and less often massive (Fig. 9a).

Magnetite was extremely rare on its own, most often it coexisted with glass, taking skeletal-dendritic forms (Fig. 8b) and polyhedrons (Fig. 9b). In the formation of crystal morphology, the internal structure plays an important role, as well as external factors, e.g., growth temperature or the degree of supersaturation. Crystals formed at low supersaturation are in the form of polyhedra. As spinels crystallize in the 48-face class, crystals in the shape of octahedron (111) are the predominant form (Bolewski and Manecki, 1984). This form was observed with the same frequency in both WKM and WBM samples. At higher pressures, skeletal crystals are formed, at the highest supersaturations dendritic forms are obtained (Sunagawa, 1987), observed mainly in the WKM sample with a larger particle diameter. Dendrites usually grow very quickly. In WKM, iron sulphides were sporadically observed between spinels, probably as pyrrhotite, as indicated by the yellow colour and reflectance value $R < 40\%$ (Fig. 8 d, e). It is possible that the particles were not in the combustion chamber long enough, or that the amount of oxygen was insufficient and the sulfides did not transform. In an oxidizing atmosphere, if the temperature is appropriate, sulphides are burned. The course of this process depends on the amount of oxygen supplied. The oxidation reaction occurs parallelly with the thermal dissociation of the mineral. In the case of coarser graining, the breakdown of pyrite may be inhibited or occur in higher temperatures, because the diffusion of gases from larger particles will be impeded (Strzałkowska, 2019). This would explain why iron sulfides were found in the material that passed through the combustion chamber. Often, on the outer surface of the particles, characteristic red internal reflections were observed, indicating a partial oxidation of the spinel surface and the transition to hematite (Fig. 9 d, e). The hematite spheres in the tested samples were smaller than the magnetite spheres and reached a maximum size of 40 µm. Hematite also appeared in the form of small lamellae (white, often with a bluish shade, brighter than magnetite) coexisting with magnetite (Fig. 8d, f). In both samples, fragments of ferrospheres were also observed, which probably came from crushing

Table 2

The value of the enrichment factor for selected trace elements.

Pierwiastek	cWK	cWKM	EF	KWK	EF _k	cWB	cWBM	EF	KWB	EF _k
Mn [ppm]	542	2092	3.9	430	4.9	464	774	1.7	550	1.4
Co [ppm]	37.7	89.4	2.4	37	2.4	42	138	3.3	26	5.3
Nd [ppm]	53.5	270.1	5.1	no data	?	90.6	200.8	2.2	no data	?
Cu [ppm]	59.8	148.5	2.5	110	1.35	56.5	839	14.8	74	11.3
Ni [ppm]	101	980	9.7	100	9.8	114	1049	9.2	52	20.2
Au [ppb]	<0.5	8.2	>16	24	0.34	<0.5	15.9	>32	20	0.8

where:

$$EF = \frac{cWKM}{cWK} \text{ or } EF = \frac{cWBM}{cWB}$$

$$EF_k = \frac{cWKM}{KWK} \text{ or } EF_k = \frac{cWBM}{KWB}$$

EF - the enrichment factor of the component in the magnetic fraction

EF_k - the enrichment factor of the component compared to the Clark

cWKM - the concentration of an element in the WKM

cWBM - the concentration of an element in the WBM

cWK - the concentration of an element in the WK

cWB - the concentration of an element in the WB

KWK / KWB - the value of the Clark of the researched element

Bold indicates that results.

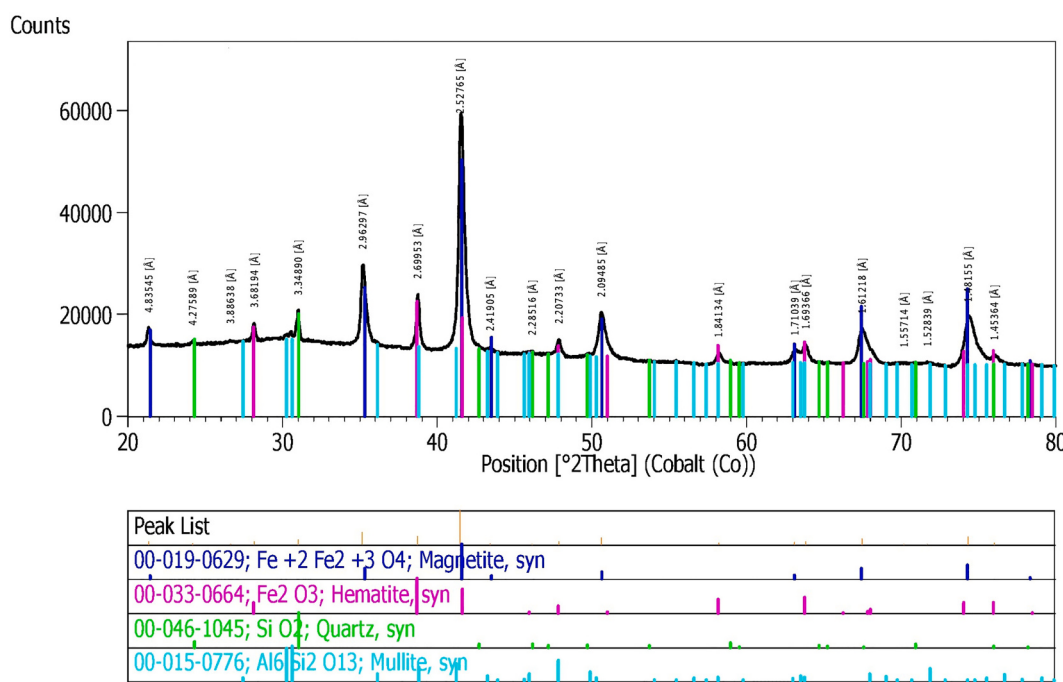


Fig. 6. X-ray diffractogram of sample WKM.

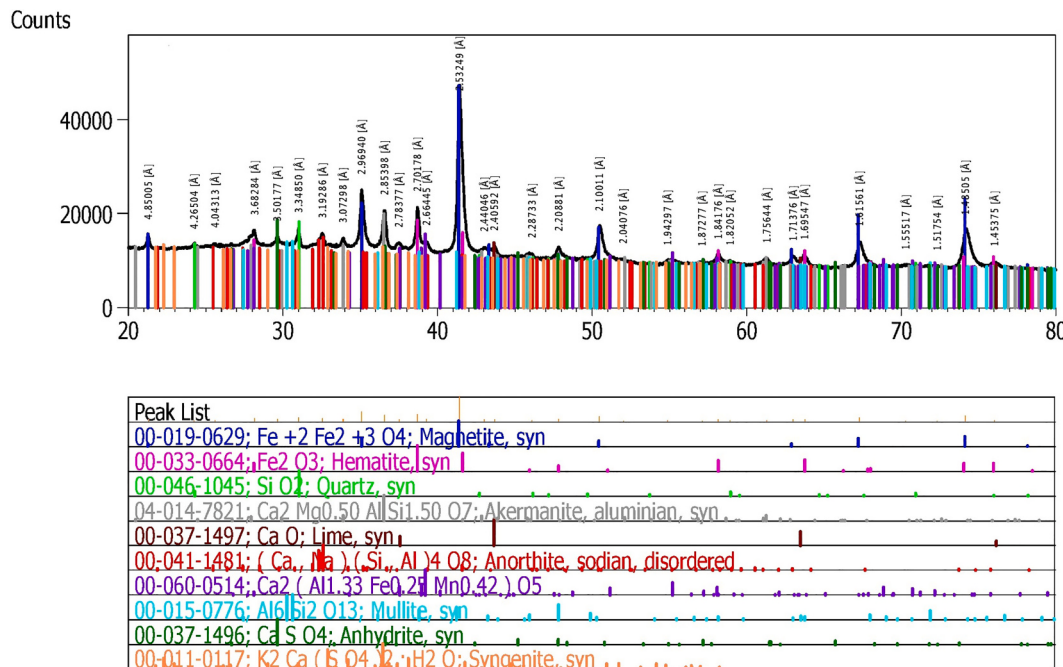


Fig. 7. X-ray diffractogram of sample WBM.

the hollow forms (Fig. 8c, f and 9c, f). In larger aggregates, the zonal structure of spinels was noticeable. Different shades of colour indicated a variable chemical composition of these aggregates (Fig. 8e).

3.5. Results of SEM-EDS analysis

In order to investigate the differences in the chemical composition of individual magnetic particles of ash and to find the answer to the question why the material, whose content of iron was lower, enriched more efficiently, the SEM-EDS analysis was performed. The chemical composition was determined in randomly selected micro-areas,

examples of the analysed particles are presented in Fig. 10. In total, 80 micro-areas were tested.

The chemical composition of the tested particles is illustrated in the box and whisker plot (Figs. 11 and 12), which is a convenient way to graphically represent a group of numbers by providing five important pieces of information: the minimum, the first quartile (Q_1), the median (Q_2), the third quartile (Q_3), and the maximum.

The analysis of the obtained results showed that the third quartile Q_3 for WBM is 91%, and the median $Q_2 = 77\%$, while in the WKM these values are lower: $Q_3 = 83\%$ and the median $Q_2 = 71\%$. Thus, the magnetic fraction of lignite coal has particles richer in Fe, therefore a

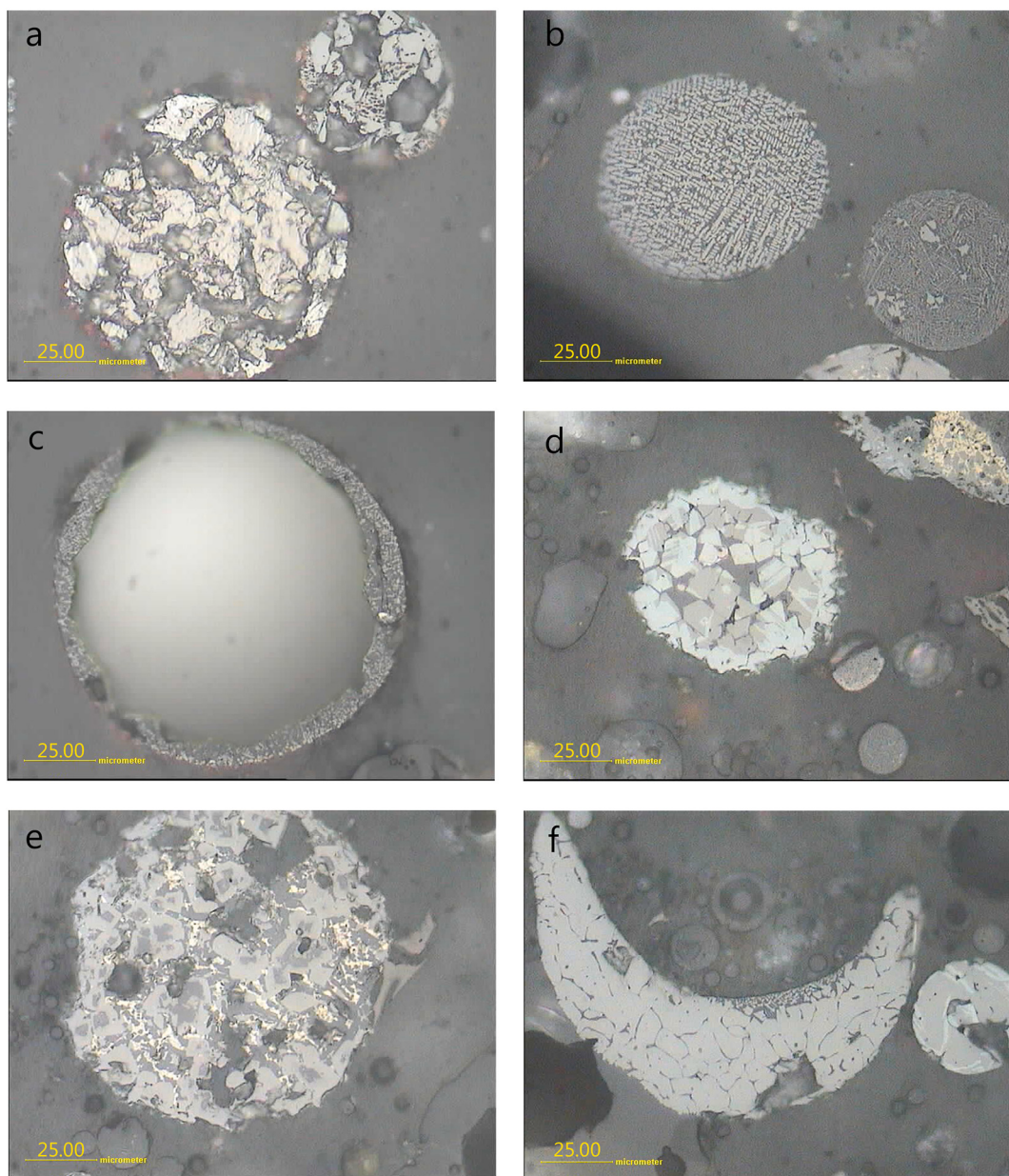


Fig. 8. Magnetic fraction of WKM a) spherical porous aggregates, b) ferrospheres of dendritic-skeletal structure c) hollow ferrosphere d) magnetite sphere (advanced stage of martitization) (white fields); on the right, spinel with iron sulphides (yellow fields) e) zonal spinel and iron sulphides (yellow fields) f) fragment of the hollow magnetic sphere. Microscopic analysis in reflected light, 1 N. (For interpretation of the references to colour in this figure legend, the reader is referred to the web version of this article.)

higher content of Fe (9%) was found in the raw material of WB than in WK (5%). Particles with such a high iron content are easily enriched. Meanwhile, the Q₁ quartile for WKM is 51%, while for WBM Q₁ = 43%. If we take the minimal observation for both samples into account, we notice that 25% of the particles in WKM have an iron content in the range of 23–51%, and in WBM 25% are iron-poor particles (4–43%). This fact may be another explanation why, despite the higher Fe content in the WB raw material compared to WK, we obtained a worse enrichment effect in the WBM sample. Probably the vast majority of the low iron particles were not enriched and remained in the non-magnetic fraction.

As the main chemical components, apart from Fe₂O₃, were: SiO₂, Al₂O₃, CaO, and MgO, the next step was to investigate the coexistence of these components in individual particles. Ternary diagrams were drawn in the following combinations: Fe₂O₃ - SiO₂ - Al₂O₃, Fe₂O₃ - SiO₂ - CaO,

and Fe₂O₃ - SiO₂ - MgO (Fig. 13).

The vertices of the triangle reflect the chemical composition of a 100% single component particle, while inside the triangle there are points reflecting the multicomponent particles. As expected, most of the points gather around the Fe₂O₃ vertex as most of the grains are iron oxides. EDS analyses reveal that some particles of the magnetic fraction have a rich glass matrix (Fig. 13). With the decrease in Fe content in the WKM particles, the Si content increases, but the Al content remains constant (Fig. 13 a), as is the Mg content in both samples. The largest dispersion of the results is observed for WBM particles with the following compositions: Fe₂O₃ - SiO₂ - Al₂O₃ and Fe₂O₃ - SiO₂ - CaO (Fig. 13 d and 13 e). It is in this group that we observe the iron-poorest particles. Probably a significant part of the particles of this group was not enriched and remained in the non-magnetic fraction. The content of MgO in WKM particles is higher than in WBM (Fig. 13c and f). These

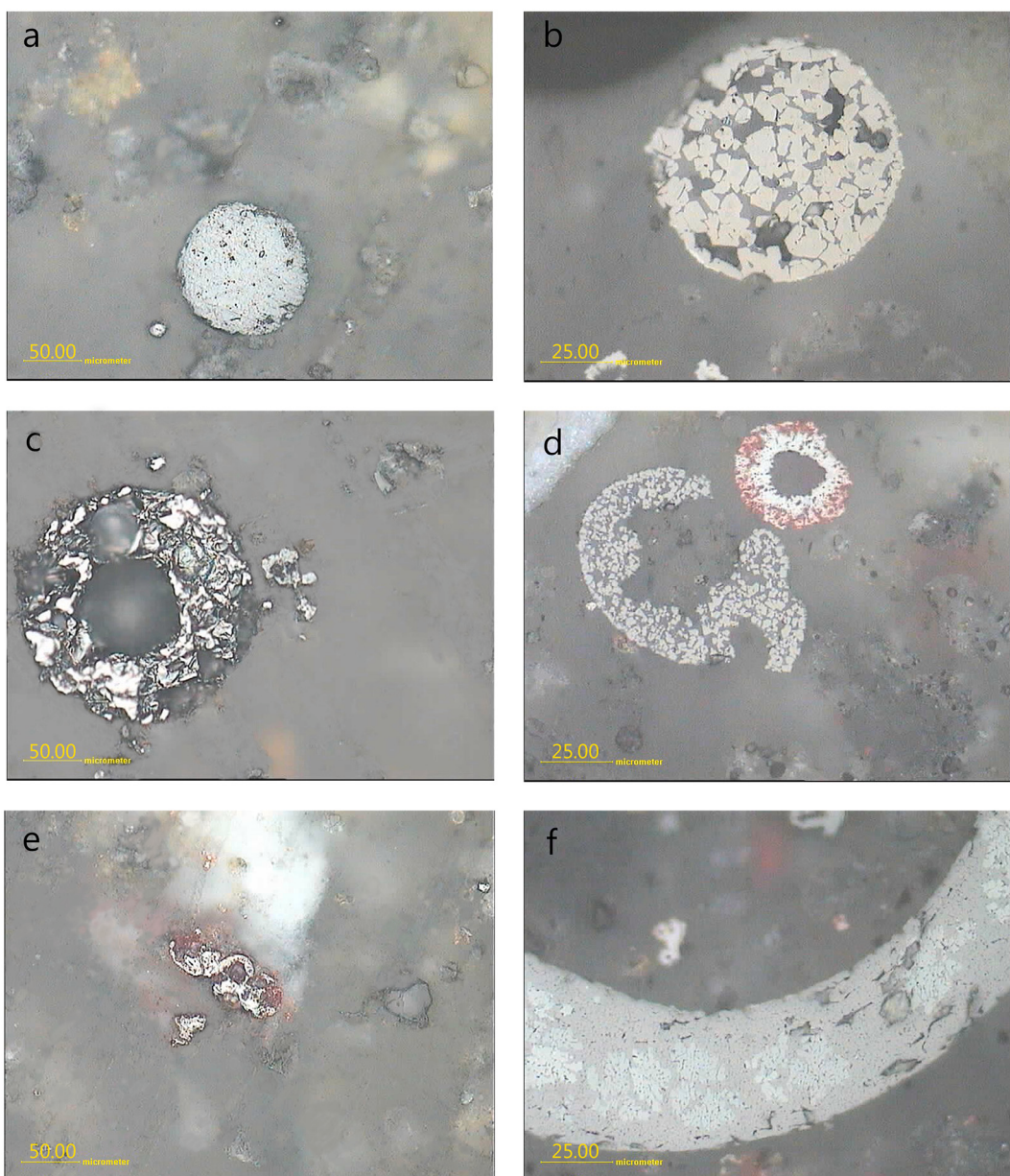


Fig. 9. Magnetic fraction of WBM a) massive magnetite b) different geometric forms of magnetite (white fields) in glass (grey field), c) hollow ferrosphere, d) different geometric forms of magnetite, on the right - hematite, visible red internal reflections e) surface oxidation of magnetite to hematite f) hollow magnetic spherules - beginning of magnetite martitization (white fields). Microscopic analysis in reflected light, 1 N. (For interpretation of the references to colour in this figure legend, the reader is referred to the web version of this article.)

particles represent magnesioferrites, which occur most often in the form of 5 to 10 μm octahedrons (Figs. 14 and 15). Such euhedral shapes suggest that they were the first to crystallize from the alloy. The space between them is of a calcium-aluminosilicate character, thus close to melilite or anorthite. Magnesioferrites are among magnetite spinels and have been extensively discussed by Valentim et al. (2018). As the formation of skeletal forms is favoured by large crystal sizes, dendritic-skeletal forms of ferrites were observed only in the WKM fraction, characterized by a coarser grain size. The basic glass was often of aluminosilicate or calcium-aluminosilicate character (Fig. 16).

Studies in micro-areas confirmed the results of microscopic observations. The analyses clearly indicate the presence of: magnetite, hematite and multicomponent phases, often trapped in an aluminosilicate glass or calcium-aluminosilicate glass.

4. Conclusions

The conducted research allowed for the formulation of the following conclusions:

- Fly ash is a source of morphologically and mineralogically diverse magnetic particles that are easy to isolate using magnetic separation. The type of coal burned, as well as the reactions taking place in the boiler between the organic substance and the mineral components of coal, have a large influence on the chemical and mineralogical differentiation of magnetic particles.
- The sizes of the magnetic particles range from 1 μm to more than 200 μm , with most of the particles being in the range of 40 to 100 μm . In the tested material, the magnetic fraction of hard coal ash is characterized by coarser grain size and higher sphericity of particles.

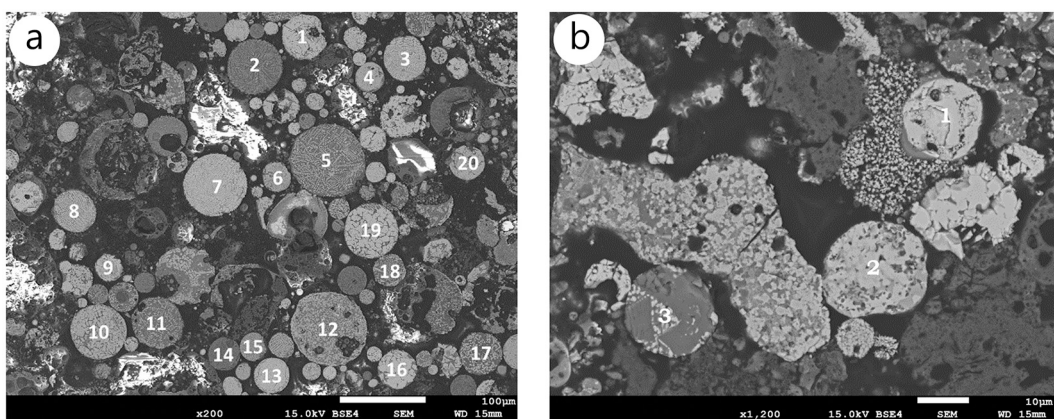


Fig. 10. Examples of ferrospheres in which the chemical composition was measured a) WKM b) WBM.

Table 3
Results of quantitative phase analysis.

Sample	Identified phase components	Content [wt%.]
WKM	Magnetite Fe_3O_4	$41,4 \pm 0,9$
	Hematite $\alpha\text{-Fe}_2\text{O}_3$	$10,9 \pm 0,9$
	Quartz SiO_2	$2,0 \pm 0,4$
	Mullite $\text{Al}_6\text{Si}_2\text{O}_{13}$	$3,3 \pm 1,3$
	Amorphous component	$42,4 \pm 4,0$
WBM	Magnetite Fe_3O_4	$31,5 \pm 0,9$
	Hematite $\alpha\text{-Fe}_2\text{O}_3$	$9,9 \pm 0,9$
	Quartz SiO_2	$1,2 \pm 0,4$
	Akermanite $\text{Ca}_2\text{Mg}_{0,5}\text{AlSi}_{1,5}\text{O}_7$	$7,1 \pm 0,9$
	Brownmillerite $\text{Ca}_2(\text{Al}_{1,33}\text{Fe}_{0,25}\text{Mn}_{0,42})\text{O}_5$	$3,5 \pm 0,9$
	Anorthite $(\text{Ca},\text{Na})(\text{Si},\text{Al})_4\text{O}_8$	$5,5 \pm 0,9$
	Lime CaO	< 1,0
	Mullite $\text{Al}_6\text{Si}_2\text{O}_{13}$	< 1,0
	Anhydrite CaSO_4	$1,1 \pm 0,4$
	Syngenite $\text{K}_2\text{Ca}(\text{SO}_4)_2 \text{H}_2\text{O}$	< 1,0
	Amorphous component	$38,4 \pm 4,4$

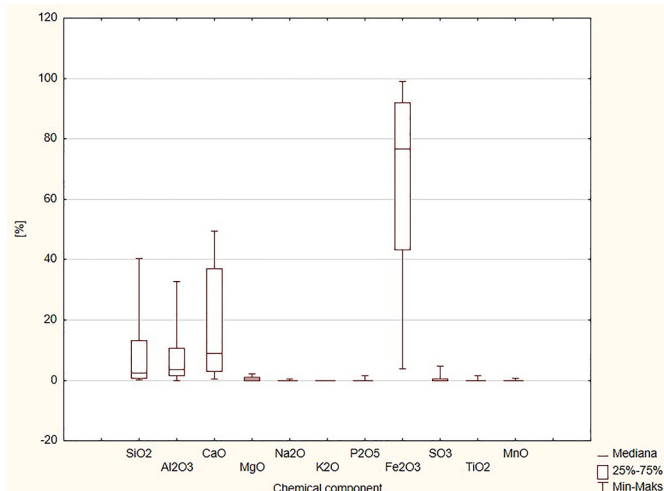


Fig. 12. Chemical composition of individual WBM particles based on SEM-EDS tests.

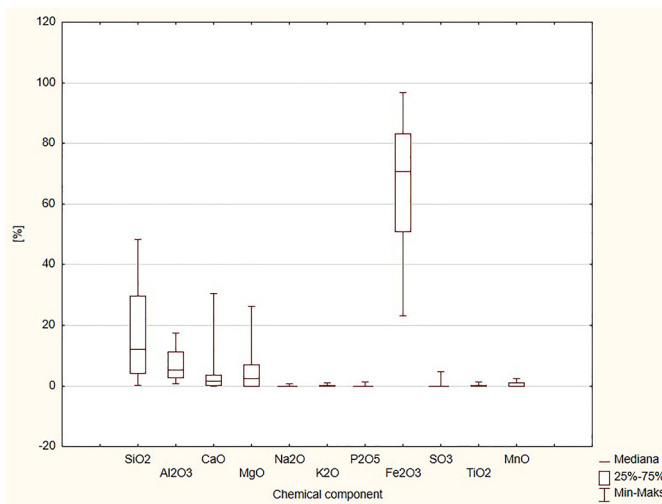


Fig. 11. Chemical composition of individual WKM particles based on SEM-EDS tests.

- When selecting the raw material for the separation of metal concentrates, the most important factor is not always the metal content in the ash, but the form of its presence. A richer concentrate was obtained from ash with a lower iron content.
- The main iron-bearing phases are magnetite and hematite, and minorly brownmillerite in the WBM sample. The lack of purity of the

magnetic fraction of both ashes can be attributed to the presence of glass particles coexisting with spinels. The glass is most often aluminosilicate or calcium-aluminosilicate. The ferrous phases with a dendritic, skeletal or polygons structure are trapped in the glass.

- The share of iron oxides and glass in particles is very variable, this variability is especially noticeable in the magnetic fraction of lignite ash. The presence of multicomponent particles will definitely lower the density of the magnetite dust. In order to determine the profitability of iron recovery from such material, prior quantitative analyses are necessary to determine the percentage of these multicomponent particles.
- The elements Mn, Co, Nd, Cu, Ni and Au were also significantly enriched, which was favoured by the internal structure of the ferrite crystal lattice.
- The high value of the enrichment factor in relation to the Cu Clark and Ni Clark for the magnetic fraction of lignite ash confirms the importance of this ash as a potential source of the above-mentioned elements.
- After the magnetic material is removed from the fly ash, the remaining product may be useful in the production of refractories and ceramics because it contains significant amounts of aluminum and silicon oxides.

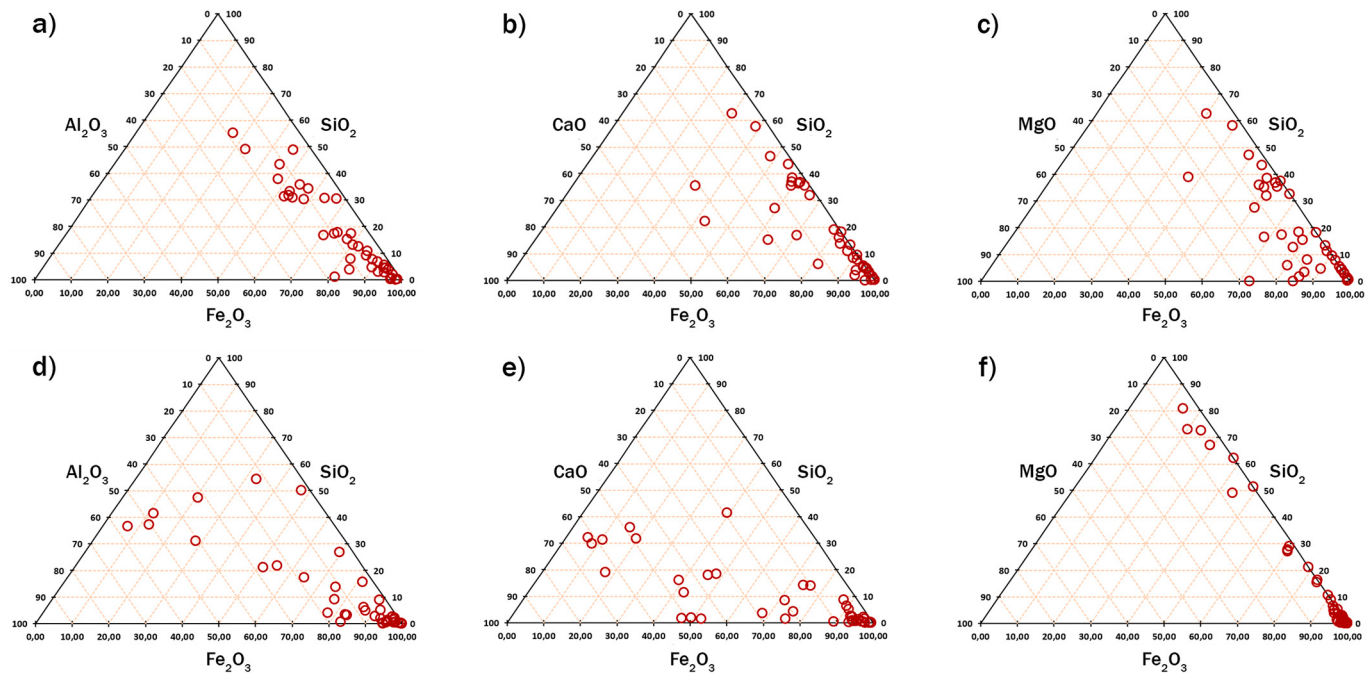


Fig. 13. Ternary diagrams for WKM (a,b,c) and WBM (d,e,f).

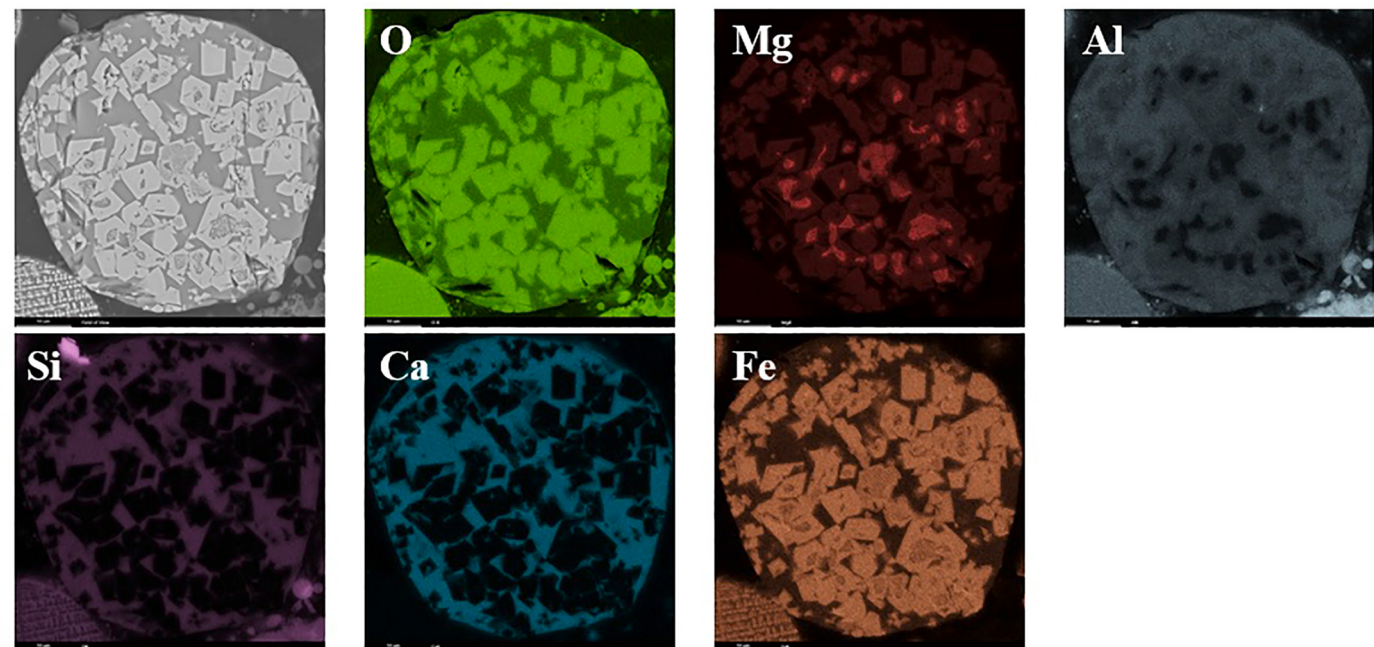


Fig. 14. Map of chemical elements distribution in the particle of WKM.

Notation

WB	Fly ash from lignite combustion (Class „C”)
WK	Fly ash from bituminous coal combustion (Class „F”)
WBM	magnetic fraction from lignite combustion
WKM	magnetic fraction from bituminous coal combustion
EDS	Energy Dispersive Spectroscopy
SEM	Scanning Electron Microscope
LOI	Loss on ignition
AR	Aspect Ratio
EF	the enrichment factor

EF_k the enrichment factor of the component compared to the Clark

Author statement

The author of the article entitled “Morphology, chemical and mineralogical composition of magnetic fraction of coal fly ash” has seen and approved the final version of the manuscript being submitted.

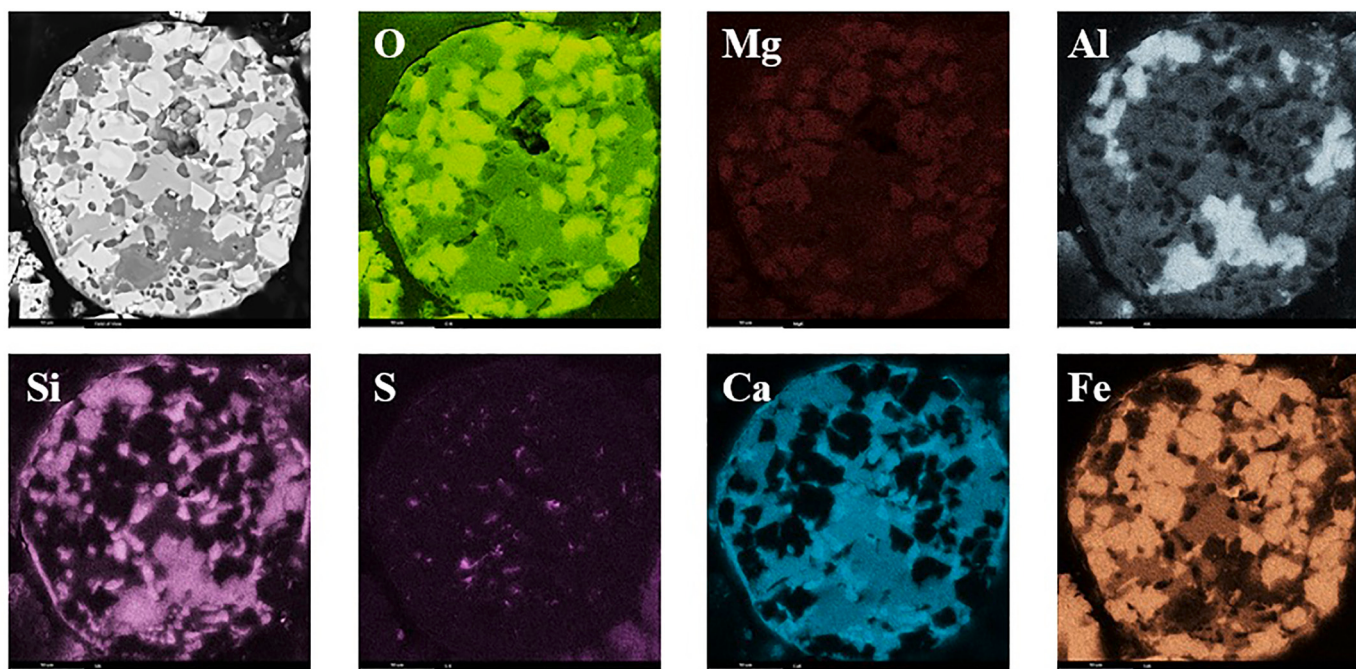


Fig. 15. Map of chemical elements distribution in the particle of WBM.

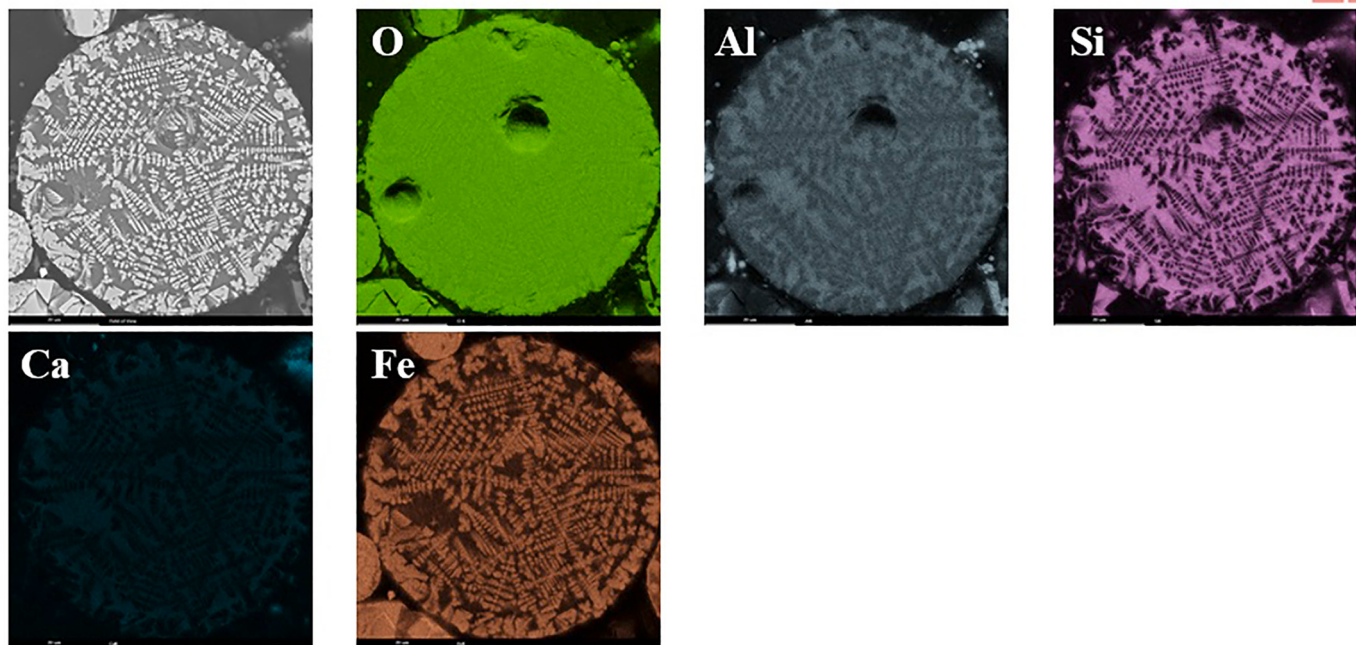


Fig. 16. Map of chemical elements distribution in the particle of WKM.

Declaration of Competing Interest

The authors declare that they have no known competing financial interests or personal relationships that could have appeared to influence the work reported in this paper.

Acknowledgements

The author thanks Atest company for measuring the size and shape of magnetic fly ash fraction using a QICPIC sensor from Sympatec GmbH.

The article has been written as a result of a research project financed

by Silesian University of Technology, Faculty of Mining, Safety Engineering and Industrial Automation from the funds of the Ministry of Science and Higher Education (BK305/RG6/2020;06/060/BK_20/0091).

References

- Adamczyk, Z., Komorek, J., Bialecka, B., Nowak, J., Klupa, A., 2020. Assessment of the potential of polish fly ashes as a source of rare earth elements. *Ore Geol. Rev.* 124 (103638), 1–17. <https://doi.org/10.1016/j.oregeorev.2020.103638>.
- Ahmaruzzaman, M., 2010. A review on the utilization of fly ash. *Prog. Energy Combust. Sci.* 36, 327–363.

- Anshits, A.G., Kondratenko, E.V., Fomenko, E.V., Kovalev, A.M., Bajukov, O.A., Salanov, A.N., 2000. Catalytic properties of active phase of glass crystal microspheres in the reaction of methane oxidation. *Stud. Surf. Sci. Catal.* 130, 3789–3794.
- Bielowicz, B., Botor, D., Misiak, J., Wagner, M., 2018. Critical elements in fly ash from the combustion of bituminous coal in major polish power plants. *E3S Web Conf.* 35 <https://doi.org/10.1051/e3sconf/20183502003>.
- Blissett, R.S., Rowson, N.A., 2012. A review of the multi-component utilisation of coal fly ash. *Fuel* 97, 1–23. <https://doi.org/10.1016/j.fuel.2012.03.024>.
- Bolewski, A., Manecki, A., 1984. Mineralogia Opisowa. AGH, Kraków.
- Dai, S., Wang, X., Seredin, V.V., Hower, J.C., Ward, C.R., O'Keefe, J.M.K., Huang, W., Li, T., Li, X., Liu, H., Xue, W., Zhao, L., 2012. Petrology, mineralogy, and geochemistry of the Ge-rich coal from the Wulantuga Ge ore deposit, Inner Mongolia, China: new data and genetic implications. *Int. J. Coal Geol.* 90–91, 72–99.
- Dai, S., Seredin, V.V., Ward, C.R., Jiang, J., Hower, J.C., Song, X., Jiang, Y., Wang, X., Gornostaeva, T., Li, X., Liu, H., Zhao, L., Zhao, C., 2014. Composition and modes of occurrence of minerals and elements in coal combustion products derived from high-Ge coals. *Int. J. Coal Geol.* 121, 79–97. <https://doi.org/10.1016/j.coal.2013.11.004>.
- De Boom, A., Degrez, M., Hubaux, P., Lucion, Ch., 2011. MSWI boiler fly ashes: magnetic separation for material recovery. *Waste Manag.* 31 (7), 1505–1513. <https://doi.org/10.1016/j.wasman.2011.01.002>.
- Enders, M., 1996. The CaO distribution to mineral phases in a high calcium fly ash ash from Eastern Germany. *Cem. Concr. Res.* 26 (2), 243–251. [https://doi.org/10.1016/0008-8846\(95\)00211-1](https://doi.org/10.1016/0008-8846(95)00211-1).
- Finkelman, R.B., Dai, S., French, D., 2019. The importance of minerals in coal as the hosts of chemical elements: a review. *Int. J. Coal Geol.* 212, 103251. <https://doi.org/10.1016/j.coal.2019.103251>.
- Flanders, P.J., 1994. Collection, measurements and analysis of airborne magnetic particulates from pollution in the environment. *J. Appl. Phys.* 75, 5931–5936.
- Gabzdyl, W., 1987. *Petrografia Węgla. Dział Wydawnictw Politechniki Śląskiej*. Gliwice.
- Galos, K., Uliasz-Bochenický, A., 2005. Źródła i użytkowanie popiółów lotnych ze spalania węgli w Polsce. *Gospodarka Surowcami Mineralnymi - Min. Resour. Manag.* 21 (1), 23–42 (in Polish).
- Giergiczy, Z., Gawlicki, M., 2005. Popiół lotny do betonu – nowelizacja normy EN 450. Budownictwo, Technologie, Architektura 3, 34–37 (in Polish).
- Giergiczy, Z., Garbacić, A., Ostrowski, M., 2013. Roads and Bridges–Drogi i Mosty, 12, pp. 71–81. <https://doi.org/10.7409/rabdym.013.006>.
- Hood, M.M., Taggart, R.K., Smith, R.C., Hsu-Kim, H., Henke, K.R., Graham, U., Groppe, J.G., Unrine, J.M., Hower, J.C., 2017. Rare earth element distribution in fly ash derived from the fire clay coal, Kentucky. *Coal Combust. Gas. Prod.* 9, 22–33. <https://doi.org/10.4177/CCGP-D-17-00002.1>.
- Hower, J.C., Rathbone, R.F., Robertson, J.D., Peterson, G., Trimble, A.S., 1999. Petrology, mineralogy, and chemistry of magnetically-separated sized fly ash. *Fuel* 78, 197–203.
- Hower, J.C., Groppe, J.G., Henke, K.R., Graham, U.M., Hood, M.M., Joshi, P., Preda, D. V., 2017. Ponded and Landfilled Fly Ash as a Source of Rare Earth Elements from a Kentucky Power Plant: Coal Combustion & Gasification Products. <https://doi.org/10.4177/CCGP-D-17-00003.1>.
- [http://EUR-Lex - 52020DC0474 - EN - EUR-Lex \(europa.eu\). 2021](http://EUR-Lex - 52020DC0474 - EN - EUR-Lex (europa.eu). 2021).
- Hulett, L.D., 1980. Chemical species in fly ash from coal-burning power plant. *Science* 1356–1358.
- Hycnar, J., 1987. Metody wydzielania koncentratów metali z popiołów elektrownianych. *Fizykochemiczne Problemy Mineralurgii* 19, 243–257 (in Polish).
- Hycnar, J.J., Kochański, B., Tora, B., 2012. Manufacture and Properties of Magnetite Dust from by-Products of Carbon Combustion. *Inżynieria Materiałowa Journal of the Polish Mineral Engineering Society*.
- Jonczy, I., Nowak, J., Porszke, A., Strzałkowska, E., 2012. Składniki fazowe wybranych mineralnych surowców odpadowych w obrazach mikroskopowych. In: *Phase Components of Selected Mineral Waste Materials in Microscope Images*. Wydawnictwa Politechniki Śląskiej, Gliwice, Monografia.
- Kabata-Pendias, A., Pendias, H., 1999. Biogeochemia Pierwiastków Śladowych. Wydawnictwo Naukowe PWN, Warszawa.
- Ketrus, M.P., Yudovich, Ya.E., 2009. Estimations of Clarkes for Carbonaceous biolithes: world averages for trace element contents in black shales and coals. *Int. J. Coal Geol.* 78, 135–148.
- Kolker, A., Scott, C., Hower, J.C., Vazquez, J.A., Lopano, C.L., Dai, S., 2017. Distribution of rare earth elements in coal combustion fly ash, determined by SHRIMP-RG ion microprobe. *Internat. J. Coal Geol.* 184 (1), 1–10. <https://doi.org/10.1016/j.coal.2017.10.002>.
- Komraus, J.L., Smolka-Danielowska, D., Wypych, E., 2003. Związki żelaza w popiołach lotnych. *Zeszyty Naukowe Politechniki Śląskiej. Seria: Górnictwo*, z 256, 125–129.
- Kukier, U., Ishak, Ch.F., Sumner, M.E., Miller, W.P., 2003. Composition and element solubility of magnetic and non-magnetic fly ash fractions. *Environ. Pollut.* 123 (2), 255–266. [https://doi.org/10.1016/S0269-7491\(02\)00376-7](https://doi.org/10.1016/S0269-7491(02)00376-7).
- Liu, P., Wang, Q., Jung, H., Tang, Y., 2020. Speciation, distribution, and mobility of hazardous trace elements in coal fly ash: insights from Cr, Ni, and Cu. *Energy Fuel* 34 (11), 14333–14343.
- Lu, S.G., Chen, Y.Y., Shan, H.D., Bai, S.Q., 2009. Mineralogy and heavy metal leachability of magnetic fractions separated from some Chinese coal fly ashes. *J. Hazard. Mater.* 169 (1–3), 246–255. <https://doi.org/10.1016/j.jhazmat.2009.03.078>.
- Martinez-Tarazona, M., Spears, D., 1996. The fate of trace elements and bulk minerals in pulverized coal combustion in a power station. *Fuel Process. Technol.* 47, 79–92.
- Michałiková, F., Bügel, M., Zelenák, F., 1994. Przeróbka popiołów z węgla kamiennego metodą flotacji i separacji na mokro w słabym polu magnetycznym. In: XII Międzynarodowy Kongres Przeróbki Węgla, Kraków 23–27 maja 1994 Kraków, pp. 227–237.
- Mishra, V., Chakravarty, S., Finkelman, R.B., Varma, A.K., 2019. Geochemistry of rare earth elements in lower Gondwana coals of the Talchir Coal Basin, India. *J. Geochem. Explor.* 204, 43–56. <https://doi.org/10.1016/j.gexplo.2019.04.006>.
- Ratajczak, T., Piestrzynski, A., 2000. Wzbogacanie magnetyczne popiołów lotnych jako metoda odzyskania i możliwości identyfikacji niektórych ich składników. *Zeszyty Naukowe Politechniki Śląskiej*, seria Górnictwo z 245, 143–157 (in Polish).
- Seredin, V.V., 1996. Rare earth element-bearing coals from the Russian Far East deposits. *Int. J. Coal Geol.* 30 (1–2), 101–129. [https://doi.org/10.1016/0166-5162\(95\)00039-9](https://doi.org/10.1016/0166-5162(95)00039-9).
- Seredin, V.V., 2007. Distribution and formation conditions of noble metal mineralization in coal-bearing basins. *Geol. Ore Depos.* 49 (1), 1–30. <https://doi.org/10.1134/S1075701507010011>.
- Seredin, V.V., Dai, S., 2014. The occurrence of gold in fly ash derived from high-Ge coal. *Mineral. Deposita* 49 (1). <https://doi.org/10.1007/s00126-013-0497-9>.
- Sharonova, O.M., Anshits, N.N., Solovyov, L.A., Salanov, A.N., Anshits, A.G., 2013. Relationship between composition and structure of globules in narrow fractions of ferrospheres. *Fuel* 111, 332–343. <https://doi.org/10.1016/j.fuel.2013.03.059>.
- Sokol, E.F., Kalugin, V.M., Nigmatulina, E.N., Volkova, N.I., Frenkel, A.E., Maksimowa, N.V., 2002. Ferrospheres from fly ashes of Chelyabinsk coals: chemical composition, morphology and formation conditions. *Fuel* 81, 867–876. [https://doi.org/10.1016/S0016-2361\(02\)00005-4](https://doi.org/10.1016/S0016-2361(02)00005-4).
- Strzałkowska, E., 2011. Charakterystyka właściwości fizykochemicznych i mineralogicznych wybranych ubocznych produktów spalania węgla. In: *Monografia, Gliwice : Wydaw. Śląskiej Politechniki* (in Polish).
- Strzałkowska, E., 2019. Analiza termiczna mineralów, skał i mineralnych surowców odpadowych. In: *Thermal Analysis of Minerals, Rocks and Mineral Waste Materials. Wydawnictwo Politechniki Śląskiej. Monografia* (in Polish).
- Suárez-Ruiz, I., Valentim, B., Borrego, A.G., Bouzinos, A., Flores, D., Kalaitzidis, S., Malinconico, M.L., Marques, M., Misz-Kennan, M., Predeanu, G., Montes, J.R., Rodrigues, S., Siavalas, G., Wagner, N., 2017. Development of a petrographic classification of fly-ash components from coal combustion and co-combustion. (An ICCP Classification System, FlyAsh Working Group – Commission III). *Int. J. Coal Geol.* 183 (1), 188–203. <https://doi.org/10.1016/j.coal.2017.06.004>.
- Sunagawa, I., 1987. In: Sunagawa, I. (Ed.), *Morphology of Minerals, [w:] Morphology of Crystals*, p. 511. Part B, Chap. 7, Dordrecht-Tokyo.
- Uliasz-Bochenický, A., Mazurkiewicz, M., Mokrzycki, E., 2015. Fly ash from energy production – a waste, byproduct and raw material. *Gospodarka Surowcami Mineralnymi – Min. Resour. Manag.* 31 (4), 139–150. <https://doi.org/10.1515/goso-2015-0042>.
- Valentim, B., Bialecka, B., Gonçalves, P.A., Guedes, A., Guimarães, R., Crucero, M., Calus-Moszko, J., Popescu, L.G., Predeanu, G., Santos, A.C., 2018. Undifferentiated inorganics' in coal fly ash and bottom ash: calcispheres, magnesiocalcisphere, and magnesiaphosphates. *Minerals* 8, 140. <https://doi.org/10.3390/min8040140>.
- Vassilev, S.V., Vassileva, C.G., 1997. Geochemistry of coals, coal ashes and combustion wastes from coal-fired power stations. *Fuel Process. Technol.* 51 (1–2), 19–45. [https://doi.org/10.1016/S0378-3820\(96\)01082-X](https://doi.org/10.1016/S0378-3820(96)01082-X).
- Vassilev, S.V., Vassileva, C.G., 2007. A new approach for the classification of coal fly ashes based on their origin, composition, properties, and behaviour. *Fuel* 86, 1490–1512.
- Vassilev, S.V., Menendez, R., Borrego, A.G., Diaz-Somoano, M., Martinez-Tarazona, M.R., 2004. Phase-mineral and chemical composition of coal fly ashes as a basis for their multicomponent utilization. 3. Characterization of magnetic and char concentrates. *Fuel* 83 (11–12), 1563–1583. <https://doi.org/10.1016/j.fuel.2004.01.010>.
- Wang, X.S., 2013. Mineralogical and chemical composition of magnetic fly ash fraction. *Environ. Earth Sci.* 71, 1673–1681.
- Wdowin, M., Franus, W., 2014. Analiza popiołów lotnych pod kątem uzyskania z nich pierwiastków ziem rzadkich. *Polityka Energetyczna – Energy Pol.* 17 (3), 369–380.
- Wei, Y., Mei, X., Shi, D., Liu, G., Li, L., Shimaoka, T., 2017. Separation and characterization of magnetic fractions from waste-to-energy bottom ash with an emphasis on the leachability of heavy metals. *Environ. Sci. Pollut. Res. Int.* 17, 14970–14979. <https://doi.org/10.1007/s11356-017-9145-8>.
- Xue, Q., Lu, S., 2008. Microstructure of ferrospheres in fly ashes: SEM, EDX and ESEM analysis. *J. Zhejiang Univ. Sci. A* 9 (11), 1595–1600. <https://doi.org/10.1631/jzus.A0820051>.